Some remarks on the Herman-Strohmer high resolution CS-radar

Tadeusz Brenner
Bumar Elektronika
tadeusz.brenner@bumar.com

Paweł Kasprzak
Bumar Elektronika and
Physics Department
Warsaw University
p.l.kasprzak@gmail.com

Leszek Lamentowski
Bumar Elektronika
leszek.lamentowski@bumar.com

***Abstract*—In this article we discuss the framework of Herman-Strohmer paper on CS-radar [4] proposing certain directions of generalizations. In particular we consider a rectangle time frequency grid of non-prime type, non-Allotop carrier signals of the length non-equal to the length of time grid, incoherent carrier and grid frequency units and the influence of $1/r^2$ decay of the amplitude of the reflected signal onto the performance of the compressed sensing algorithm. For all these generalizations we perform the numerical simulations checking the limitations of the CS-algorithm.**

I. Introduction

The signal processing technique known as the *Compressed Sensing* (CS) enables the recovery of a sparse signal on the basis of an incomplete information about it. Roughly speaking a sparse signal $x_0 \in \mathbb{R}^N$ can be recovered on the basis of a small number of measurements $b = Ax_0 \in \mathbb{R}^K$, where $K \ll N$. The precise mathematics that stands behind the above statement provides the conditions on K, N and the matrix A together with the precise formulation of the *sparseness* condition for which the recovery may be performed. Furthermore it gives rise to the probabilistic estimation for the exact recovery to occur as well as the implementable algorithms that realizes the recovery - for the details of the aforementioned mathematical issues see [1], [2] whereas for the explanation of the algorithm implementation see [3]. Soon after the discovery of the mathematical theory of the compressed sensing M.A. Herman, T. Strohmer in [4] noticed the potential application of CS for the high resolution radar. Since our paper strongly uses the framework of [4] we shall sketch its content in the next sections whereas in the next paragraph we shall briefly recall the decay character of the electromagnetic waves which we then integrate into the CS - radar.

The wave equation describing the propagation of the electromagnetic wave $(\vec{E}, \vec{B})$ is of the form

$$\left(\vec{\nabla}^2 - \frac{1}{c^2}\frac{\partial^2}{\partial t^2}\right)\vec{E} = 0$$
$$\left(\vec{\nabla}^2 - \frac{1}{c^2}\frac{\partial^2}{\partial t^2}\right)\vec{B} = 0$$

Taking an arbitrary function f one gets a $1/r$ decaying spherically symmetric solution of the electric part of the field (the magnetic part is described similarly)

$$\vec{E} = \vec{E}_+ \frac{f(r - ct)}{r}.$$

In the case of the reflection of the wave from a target we get the $1/r^2$ decay of the reflected signal amplitude. This decay character will be then integrated into CS-radar.

II. High-Resolution Radar via Compressed Sensing

In order to present the idea that lies behind the radar application of the compressed sensing we consider a certain configuration of K objects of a given distances and velocities. The data on the distance, velocity and reflection coefficient may be represented on the time-frequency plane: the distance x of a given object gives rise to the time delay variable $t = 2x/c$, the velocity v gives rise to the Doppler shift $\mu = -2v\mu_r/c$ (where μ_r is the carrier frequency) and each object is characterized by a reflection coefficient $s_{t,\mu}$. In particular $s_{t,\mu} = 0$ corresponds to the lack of an object at the point of coordinates (t, μ).

Let us now consider a radar that illuminates the space with an electromagnetic wave which is then reflected from the targets and registered by the antena. In order to perform the signal processing we introduce the time-frequency cut offs and discretize the time-frequency plane introducing the $N \times (2M + 1)$ grid - N corresponds to the time shift grid and the oddness of the number $2M + 1$ reflects the fact that the velocity may be either positive or negative or zero. Clearly the grid corresponds to the choice of time and frequency units which we denote by t_N and μ_M. The range cut off is then given by Nct_N whereas the frequency cut off is $M\mu_M$ (the frequency ranges from $-M\mu_M$ to $+M\mu_M$ while the time delay ranges from t_N to Nt_N). Note that in [4] the authors assumed N to be prime and $2M + 1 = N$, which we drop in our paper. Using the $N \times (2M+1)$ grid, the configuration of the objects, their velocities and the reflection factor is may be represented by the double index sequence $s_{kl} \in \mathbb{C}$, $k \in \{1, 2, \ldots, N\}$, $l \in \{-M, -M + 1, \ldots, +M\}$. Let us consider the periodic signal f of the period $T_r = 1/\mu_r$ that is emitted by the CS-radar. It is reflected from the objects and the echo is registered by the antenna. The reflected signal is then probed with the probing coefficient P. Using the Fourier analysis we represent the emitted signal in the form of the Fourier series:

$$f(nT_r/P) = \sum_{d=0}^{L-1} a_d e^{2\pi\imath d/T_r \cdot nT_r/P}.$$

The registered echo is the superposition of the echos reflected by the objects: the object represented by the (k, l) point on the time-frequency plane reflects the following signal

$$\frac{s_{kl}}{k^2} \sum_{d=0}^{L-1} a_d e^{2\pi\imath(d/T_r - l\mu_M)\cdot(nT_r/P - kt_N)},$$

where we put the $1/k^2$ - decay factor alluded in introduction. Absorbing the factor $e^{2\pi\imath lk\mu_M t_N}$ into s_{kl} and introducing the phase $\omega = e^{-2\pi\imath\mu_M T_r/P}$ we see that the echo of the (k, l) object measured at the n-th moment is given by

$$\frac{s_{kl}}{k^2} f((n - kPt_N/T_r)T_r/P)\omega^{nl}.$$

Defining

$$\Lambda \equiv Pt_N/T_r \tag{1}$$

we get the echo of the form

$$\frac{s_{kl}}{k^2} f((n - k\Lambda)T_r/P)\omega^{nl}. \tag{2}$$

Let us note that in the framework of the paper [4] we have $P = N$, $\omega = e^{2\pi\imath/N}$ and $\Lambda = 1$ and $T_r = Nt_N$. This mathematically convenient assumption seems to be rather difficult to justify in the context of the CS-radar application.

Having fixed the above context and ignoring T_r/P factor in (2) we see that each object provide the linear transformation of the emitted signal

$$\frac{s_{kl}}{k^2} f(n - k\Lambda)\omega^{nl}.$$

Summing up with respect to (k, l) we get the echo at the n-th probing moment

$$\sum_{kl} \frac{s_{kl}}{k^2} f(n - k\Lambda)\omega^{nl}.$$

Measuring the echo at the moments $\{n_1, n_2, \ldots, n_I\}$ where I is sufficiently large we address the problem of recovering s_{kl} out of the measured echos. Provided that s_{kl} is sufficiently sparse we shall in the next sections test the compressed sensing algorithms performance on s_{kl} recovery in our framework.

The last issue that we would like to discuss in this section is the form of the emitted signal f. In the framework of the paper [4] the authors assumed f to be of the Alltop form. Since we dropped the primness assumptions for the time grid N we had to drop the Alltop signal as well. Instead we have used the signal f which is random in the range of the period and then periodically repeated. As the general theory suggest such a signal with a high probability should give rise to the exact recovery of the targets configurations which we confirm on the level of numerical simulations.

III. Simulation results

Having the Herman-Strohmer framework analyzed and slightly extended we performed the simulations confirming the applicability of the CS-techniques in our context. Let us briefly analyze the results of the simulations referring to [5] for more details. In the simulations described below we ignored the $1/r^2$ decay factor - its influence on the CS-algorithm will be discussed in the next section.

- We performed CS-radar simulations using rectangular time-frequency grid with the non-prime time grid N. In order to do this we had to drop the Alltop signal using the random Bernoulli signal periodically repeated. The CS-algorithm performed well for the signal that is sparse enough.
- We performed CS-radar simulations using $\Lambda \neq 1$ (see Equation (2)). The CS-algorithm performed well as long as Λ and the probing coefficient P are relatively prime.
- We performed CS-radar simulations using the phase factor $\omega = e^{-2\pi\imath\mu_M T_r/P}$ with different choices of $\mu_M T_r/P$ - factor. The CS-algorithm performed well as long as ω does not generates a cyclic group of order smaller then $2M+1$.
- Finally dropped a group of measurements and register the reflected signal in randomly chosen instances. There are limitation with respect to the relative size of the dropped measurements but we checked that within a certain range the CS-algorithm performs well.

IV. CS-RADAR AND THE $1/r^2$ DECAY

In this section we shall check the influence of $1/r^2$-decay of the reflected signal amplitude onto the performance of the CS-algorithm. We consider two targets having the same reflection coefficients $s_1 = s_2 = 1$. The first object is kept in the vicinity of the radar on the time grid $n = 3$ while the position of the second object varies from 4 to 95. Using the CS-algorithms we performed the recovery of the signal using two versions of the algorithms: **Min-l_1 with bounded residual correlation** and **Min-l_1 with equality constraints** (for the details concerning the algorithms we refer to [3]). There is striking difference of the time-scale performance of the algorithms: the first needs 5sec whereas the second 120sec for the recovery of the signal. Besides this difference, both of them performs well - we attach three exemplifying figures of the recovery for each of them.

In the legend of the next figures n denotes the position of the second objects. The time grid $N = 100$ whereas the frequency grid $M = 31$.

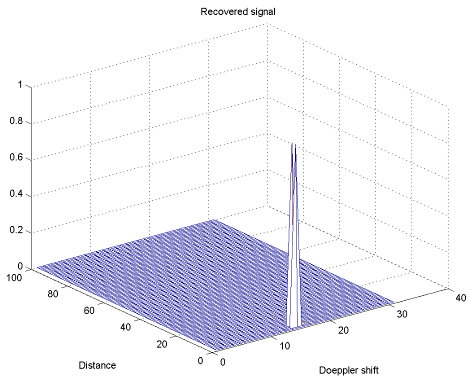

Fig. 1. Min-l_1 bounded res. corr., $n = 5$

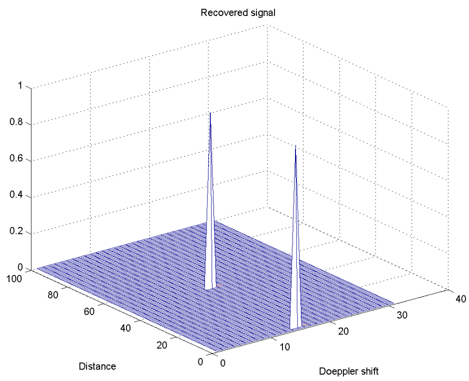

Fig. 2. Min-l_1 bounded res. corr., $n = 50$

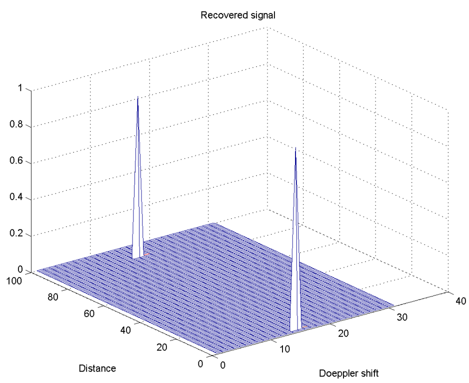

Fig. 3. Min-l_1 bounded res. corr., $n = 90$

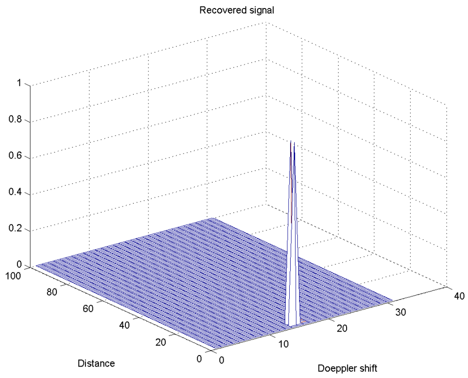

Fig. 4. Min-l_1 eq. constraints , $n = 5$

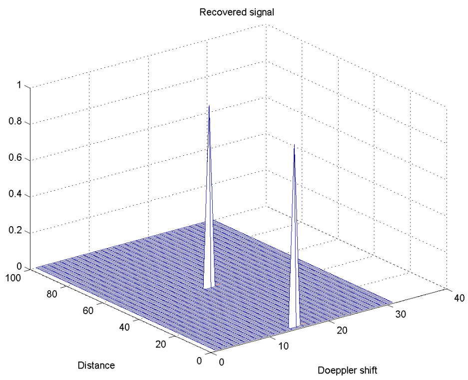

Fig. 5. Min-l_1 eq. constraints, $n = 50$

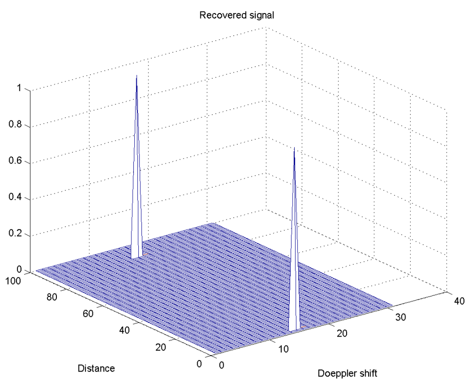

Fig. 6. Min-l_1 eq. constraints, $n = 90$

V. THE ACCURACY OF SIGNAL RECOVERY

The simulations described in previous section suggests that CS-algorithm is able to recover the sparse signal even when the numbers appearing in the signal are of the different scale: the signal from the second object when registered from the distance $N = 90$ is approximately 10^{-4} weaker then the signal from the first object. Motivated by this observation we performed the simulations focused on this issue. To be more precise we kept the first object of the reflection coefficient $s_1 = 1$ in the distance $n = 4$ whereas the second object is placed at the distance $n = 50$. The reflection coefficient of the second object varies: $s_2 = 1, 1/10, 1/100, \dots, 10^{-7}$.

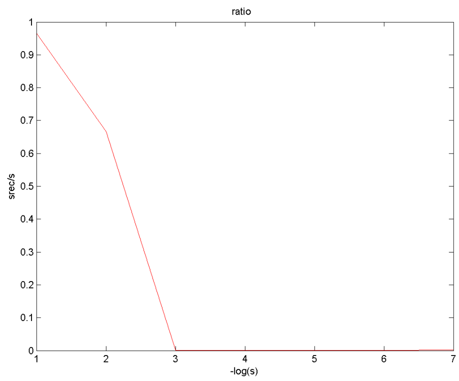

Fig. 7. Min-l_1 bounded res. corr., s_{rec}/s

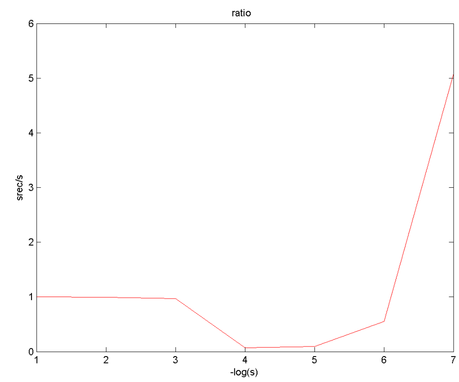

Fig. 8. Min-l_1 eq. constraints, s_{rec}/s

On the above figures we may see the ratio of the recovered signal coefficient versus the actual reflection coefficient. The X-axis represents the reflection coefficient in the inverse $\log$-scale while on the Y-axis we have the corresponding ratio. The simulation were performed for two CS-algorithms used in the previous section. We may see that the **Min-l_1 eq. constraints** performs slightly better then **Min-l_1 bounded res. corr.,** s_{rec}/s getting accurate recovery for $k = 1, 2, 3$.

References

[1] E.J. Candés, J. Romberg, T. Tao, *Robust Uncertainty Principles: Exact Signal Reconstruction From Highly Incomplete Frequency Information*, IEEE Trans. Inform. Theory, 2006, vol.52, no. 12, pp: 5406-5425.

[2] E.J. Candés, T. Tao, *Near Optimal Signal Recovery From Random Projections: Universal Encoding Strategies?*, IEEE Trans. Inform. Theory, 2006, vol. 52, no. 2, pp: 121-127.

[3] E.J. Candés, J. Romberg, l_1*-Magic: Recovery of Sparse Signals via Convex Programming*, IEEE Trans. Inform. Theory, 2006, vol. 52, no. 2, pp: 121-127.

[4] M.A. Herman, T. Strohmer, *High-Resolution Radar via Compressed Sensing*, IEEE Trans. Sig. Proc., 2009, vol. 57, no. 6, pp: 2275-2284.

[5] T. Brenner, P. Kasprzak, L. Lamentowski *Towards the realistic applications of compressed sensing in radar systems* Proceedings of SPS2013, IEEE.